

Mapping Out Protein Hydration Dynamics by Overhauser Dynamic Nuclear Polarization

Chi-Yuan Cheng, Jinsuk Song, John M. Franck and Songi Han

1 Introduction

Water molecules in the immediate vicinity of biomolecular surfaces (e.g., protein, lipid membranes, and DNA) are essential to mediate biological activities, such as enzyme activity, ligand binding, allosteric effect, or molecular recognition (Ball 2008a, b; Zhong et al. 2011). For instance, the formation of a functional enzyme-substrate complex may be mediated by the retardation of water mobility at the active site of the enzyme (Grossman et al. 2011). Hydration water could also facilitate specific protein function, such as channel gating, whose kinetics has been found to be critically correlated with the rate of water fluctuations (Rasaiah et al. 2008; Zhu and Hummer 2010; Kim et al. 2009). Additionally, water is generally thought to be a catalyst for the hydrogen-bond rearrangements of a protein (Xu and Cross 1999). The prevailing view is that water molecules actively contribute to the hydrophobic effect involved in protein-folding and ligand-binding events by modulating protein conformational changes through the formation or breaking of hydrogen bonds at protein-water interfaces (Cheung et al. 2002; Zhou et al. 2004). Interestingly, the diffusion dynamics of hydration water that entails hydrogen-bond rearrangement of the dynamic protein-water network may be critically coupled to protein dynamics, not only at the interfaces, but also at the core (Raschke 2006). A combination of the rapid hydrogen-bond rearrangements and the fast hydration dynamics at protein-water interfaces are suggested to be essential in increasing the protein structural

S. Han (✉) · C.-Y. Cheng · J. Song · J. M. Franck
Department of Chemistry and Biochemistry, University of California,
Santa Barbara, CA 93106, USA
e-mail: songi@chem.ucsb.edu

S. Han
Department of Chemical Engineering, University of California,
Santa Barbara, CA 93106, USA

© Springer Science+Business Media, LLC 2015
L. Berliner (ed.), *Protein NMR*, Biological Magnetic Resonance 32,
DOI 10.1007/978-1-4899-7621-5_2

flexibility and facilitating protein-ligand recognition (Roy and Bagchi 2012; Levy and Onuchic 2006; Fenimore et al. 2002).

In the case of membrane protein that is embedded in an environment composed of diverse lipids and biochemical species, the dynamical coupling between hydration water and protein could be more complex than in soluble protein systems (Page et al. 2007; Zhou and Cross 2013). The hydration water within the hydrophobic core of lipid bilayers distributes to form a strong, sigmoidal, concentration gradient across the bilayers (Aman et al. 2003; MacCallum and Tieleman 2011; Wimley and White 1996). The presence of these hydration water molecules within the bilayer core serve as bridges between protein's hydrogen-bonding donors and acceptors, and together with various physical forces in the low dielectric lipid environment, may yield significant energetic barriers for the conformational transformation of the protein within the lipid environment, thereby stabilizing the membrane protein structures (Dong et al. 2012). Importantly, hydration water at the solvent-exposed sites of a membrane protein may actively facilitate ligand recognition, whereas hydration water at the membrane-buried sites of a membrane protein stabilizes the protein structure. While the nature of the protein's hydration layer has been of great interest to experimentalist and theorist, its exact characteristics that differentiates its role from that of bulk water is not fully understood. Unanswered questions include how or whether the hydrogen-bonding structure or dynamics of surface hydration water differs from bulk water, what is the dynamic range and energy barrier of the extended hydration layer around a protein surface, how the molecular environments influence the properties of surface hydration water (i.e., chemistry and topology of a surface, solvent quality, ions, small molecules, etc.) that modulate this dynamic range and energy barrier for surface water diffusion, and what is the structural and dynamic property of hydration water within the hydrophobic environments of folded or partially folded proteins and the lipid bilayers.

While existing biophysical tools have provided important physical insights to the nature of protein hydration water at the molecular level and across a vast range of timescales, a more complete and unified view on protein hydration water in aqueous solutions is needed. A recently developed technique, termed Overhauser dynamic nuclear polarization (ODNP)-enhanced nuclear magnetic resonance (NMR) relaxometry, should contribute to the search for a unified understanding of protein hydration water by offering novel and alternative experimental capabilities for directly detecting the diffusion dynamics of local water at the surface or interface of biomolecules under ambient solution conditions. ODNP uniquely measures the dynamic range of protein hydration water that diffusively moves within tens to hundreds of picoseconds within 10 Å distances (2–4 hydration layers) from a stable nitroxide radical-based spin label that can probe solution environments or can be tethered to the surfaces of proteins. The strength of the ODNP approach is that it relies on NMR signal amplification, offering enhanced sensitivity, and harnesses the amplified NMR signal from site-specifically introduced spin labels or locally partitioning spin probes, thus offering site-specific or localized measurements of water dynamics on biomolecular surfaces or environments of interest. Crucially, ODNP is carried out under biologically relevant environments, i.e., in dilute solution and

of minute sample quantities, in the presence of ions and solutes if needed, and at physiological temperatures, which is otherwise a challenging environment to experimentally discern properties of surface hydration water, distinct from bulk water. Our goal of this chapter is to convey a concise review of the ODNP methods and applications that have offered a unique approach to quantify hydration dynamics in complex protein systems with spatial and temporal contrast. After briefly surveying select, existing, biophysical tools for studying protein hydration, we review the ODNP theory and experimental approaches, as well as highlight recent studies of soluble, membrane, and aggregating proteins.

1.1 *Biophysical Tools to Study Protein Hydration*

Although several experimental methods for characterizing protein hydration water have been established that are complementary with each other, they are still plagued by controversies in interpretation of the timescales and spatial extent of what is termed hydration water or biological water for many years (Halle 2004). While structural water that is strongly correlated with the polar side chains or hydrophobic cavities of a protein can be detected by X-ray crystallography with angstrom resolution (Burling et al. 1996), molecular dynamics studies suggest that it is the significant dynamic modulation of protein hydration water within picosecond timescales that is strongly associated with its biological functions (Russo et al. 2004; Tarek and Tobias 2000; Wood et al. 2007). Therefore, experimental methods that can directly probe the dynamic property of protein hydration water over a wide range of timescales, from the rapid cooperative reorganization of hydrogen-bond network in the sub-picosecond region (Vinh et al. 2011; Ebbinghaus et al. 2007; Grossman et al. 2011; King and Kubarych 2012) to the water rotational and translational diffusion in the few tens to hundreds of picosecond regime, can greatly improve our understanding of protein function. Selected examples of existing tools to study the hydration dynamics are summarized below:

- *Quasi-elastic neutron scattering (QENS)* offers a model-free approach to quantifying hydration dynamics on the picosecond to nanosecond timescale and at angstrom length resolution, yet averaged over all water populations within the sample (Svergun et al. 1998; Head-Gordon and Hura 2002; Russo et al. 2004; Tehei et al. 2007). To quantify the dynamic properties of protein hydration water, high protein concentrations (~hundreds mM) are chosen to ensure overlapping hydration shells, so that all water populations constitute protein hydration water that is characterized (Gabel et al. 2002).
- *^{17}O and ^2H magnetic relaxation dispersion (MRD)* obtains information about rotational dynamics of hydration water moving with tens of picosecond to nanosecond (magnetic dipolar) correlation times on protein surfaces, or microsecond lifetimes for buried water within the protein cavities. With this approach, a selective observation of different classes of hydration water in a protein can be achieved that contains different correlation times, by measuring the frequency

dependence (dispersion) of the T_1 relaxation rate for ^2H and/or ^{17}O isotopes of water molecules in a protein solution (Denisov 1999; Halle and Davidovic 2003; Halle 2004; Mattea et al. 2008; Persson and Halle 2008b, a; Otting et al. 1991; Gottschalk et al. 2001). While early NMR studies based on the intermolecular nuclear Overhauser effect (NOE) have reported that the hydration dynamics around protein surfaces is in the sub-nanosecond regime that would correspond to retardation factors larger than 5–10 (Otting et al. 1991), more recent observations made by MRD suggested that rotational water mobility on protein surfaces is only be retarded by a factor of 2–3 compared with bulk water mobility (Halle 2004). This reevaluation has been enabled by exploiting supercooled protein solutions to efficiently retard the mobility of the buried water, that allows for the select measurement of only the surface hydration water averaged over the entire protein surface (Mattea et al. 2008; Davidovic et al. 2009). Compared to QENS, less concentrated protein on the order of few to tens of mM can be studied by MRD, but this is still far from accessible concentrations for most biomolecular systems.

- *^1H MRD using site-specific paramagnetic spin labels*, often referred to as field cycling relaxometry (FCR), can offer measurements of site-specific hydration water dynamics by exploiting ^1H T_1 relaxation rate of hydration water induced by tethered, local, paramagnetic spin labels (Borah and Bryant 1981; Korb et al. 2006; Korb and Bryant 2001). While offering unique and quantitative information for many biological and materials surfaces, protein surfaces that tend to display significant bound water populations could make the unambiguous interpretation in terms of hydration water challenging (Diakova et al. 2010).
- *Nuclear Overhauser Effect (NOE) and rotating-frame NOE (ROE) relaxation measurements using proteins encapsulated in reverse micelles* have been recently developed to provide site-resolved information on protein hydration dynamics (Nucci et al. 2011b, a). Although early NOE studies pursued the study of site-resolved dynamics, residence time, and location of internal water molecules within the protein structure (Otting et al. 1991), it faced technical or interpretational limitations when studying the hydration water on the protein surface that is rapidly exchanging with the surrounding bulk water, complicating the interpretation of long-range dipolar coupling from bulk water in competition with hydrogen exchange effects (Halle 2003). Wand et al. have demonstrated that the encapsulation of a protein within a reverse micelle can significantly reduce the motion of hydration water and hydrogen-exchange kinetics of proteins, allowing for the dynamics of hydration water bound to the protein surface to be unambiguously resolved by solution-state NMR for the first time (Nucci et al. 2011b, a).
- *Dielectric relaxation (DR) spectroscopy* measures the frequency-dependent part of the relative permittivity in the frequency range from a few MHz to 20 GHz, which correspond to time scales that ranges from few picoseconds to microseconds (Bagchi 2005; Nandi et al. 2000). Thus, many modes of hydration water dynamics from bulk to surface-bound populations could be measured (Fenimore et al. 2004; Mazza et al. 2011).

- *2D infrared (IR) methods* can offer valuable information about the local hydration dynamics of small peptides in solutions at the femtosecond to picosecond timescale by isotope labeling a backbone with $^{13}\text{C}=^{18}\text{O}$ or a side chain with C–D, thus offering site-specific information with minimal perturbation to the peptide or protein structure (Hochstrasser 2005; Manor et al. 2009). Although the isotope labeling strategies have general limitations in large proteins, 2D-IR approaches to study hydration dynamics in large proteins using nonnative probes have been recently developed (Woys et al. 2013; King and Kubarych 2012; King et al. 2012; Lindquist et al. 2009). For example, the Kubarych group used a local metal carbonyl complex attached to a lysozyme protein surface and observed that the hydrogen-bond water dynamics is a factor of 2 slower than that of bulk water (King and Kubarych 2012).
- *Terahertz (THz) spectroscopy* has been used for measuring the global modulation of water networks on the sub-picosecond to picosecond time scale (Ebbinghaus et al. 2007; Xu et al. 2006) by measuring the differential absorption of sub- to several THz radiation by bulk versus surface hydration water in protein systems (Ebbinghaus et al. 2007; Grossman et al. 2011; Luong et al. 2011; Niehues et al. 2011; Vinh et al. 2011). The THz method has been shown to be much more sensitive to detecting fast water dynamics than relying on DR or IR spectral changes (Ronne et al. 1997). Again, the average properties of hydration water around the entire protein surface are measured and relatively high protein concentrations (mM range) are needed.
- *Time-resolved fluorescence spectroscopy* is unique in that it provides protein site-specific dynamic information about the protein hydration water at the femtosecond to hundreds of picosecond timescale by employing a single tryptophan mutant on the protein surface (Li et al. 2007; Zhang 2007; Zhang et al. 2009). The relaxation of the water network surrounding the protein surface upon electronic excitation of the tryptophan probe has been observed to include local (1–8 ps) and global (20–200 ps) rearrangements of surface hydration water, whose hydration dynamics is differentially and site-specifically retarded on protein surfaces relative to that of bulk water (Zhang 2007).

Among the above listed tools, ^1H MRD, 2D-IR, and time-resolved fluorescence spectroscopies offer unique and powerful capabilities to probe the changes of the protein hydration dynamics in the vicinity of a site-specific molecular probe on the protein or peptide surface, and that with femtosecond up to picosecond time resolution. Insight from molecular dynamics simulations and other quantitative studies (Russo et al. 2004; Tarek and Tobias 2000; Wood et al. 2007) suggest that experimental methods that can directly and unambiguously probe the protein hydration dynamics within few to tens and hundreds of picosecond time scales, with site-specificity and of dilute protein systems under biologically viable sample conditions, are highly desirable to extend the studies to a broader range of systems and desirable solution conditions, as well as to resolve spatial heterogeneities in hydration water diffusion expected on biomolecular surfaces.

1.2 Introduction to ODNP

ODNP-enhanced NMR relaxometry is a recently introduced spectroscopic method that quantifies the site-specific translational dynamics of hydration water. ODNP utilizes site-specifically tethered nitroxide spin labels on biomolecules to polarize the water protons within 10 Å distances from the spin label that rapidly move across these distances with 10–1000 ps correlation times, corresponding to translational diffusive motion of free to loosely bound water (Armstrong and Han 2007, 2009; Franck et al. 2013a). ODNP relies on efficiently transferring the higher polarization from the unpaired electron spins to dipolar-coupled protons of nearby hydration water by microwave irradiation at the electron paramagnetic resonance (EPR) frequency of the spin label, thereby enhancing the ^1H NMR signal amplitude. As this electron–proton cross relaxation is dominantly driven by dipolar coupling in solution (Borah and Bryant 1981), the effect of closer protons is most heavily weighted, with the experimentally determined distance of closest approach between the electron and proton found to be ~ 3.8 Å (Hodges et al. 1997; Franck et al. 2013a). As a result, the ^1H NMR signal of hydration water can be effectively amplified up to ~ 300 fold at 25 °C and 0.35 T that is incidentally the most common magnetic field strength for EPR spectroscopy (employing X-band EPR frequency). It has been shown that the translational diffusion dynamics of hydration water at specific sites of interest (surface and interior) on a wide range of biomolecular systems covers a large dynamic range, covering the entire correlation time regime of 10–1000 ps that can be quantified by ODNP relaxometry. ODNP methods have been shown to track protein structural rearrangements that involve the complete or partial burial of protein interfaces as part of protein folding events (Armstrong et al. 2011), protein aggregation events (Pavlova et al. 2009) or even conformational changes of membrane protein segments upon activation (Hussain et al. 2013; Hussain et al. 2015). Interestingly, ODNP-based hydration dynamics measurements not only sensitively picks out events that involve the change in the exposure or burial of protein segments, but measures variation in hydration dynamics on entirely solvent-exposed surfaces, depending on the chemical and topological make-up of the surface, types of solutes present in the solution and solvent conditions (Franck et al. 2013b). Specifically, ODNP at X-band confirms the presence of an extended dynamic hydration layer (2–4 water layer thickness; Ebbinghaus et al. 2007) with significantly retarded diffusion dynamics by 2–10 fold on protein surfaces (Cheng et al. 2013), compared to bulk water, that translates into an additional activation energy barrier imposed by the surface hydration layer relative to that of bulk water diffusion, that is up to several fold the thermal energy (Kausik et al. 2009). It also experimentally confirmed that there is a distinctly diverse hydration dynamics landscape on surfaces of protein and lipid membrane, as previously observed by other experimental techniques (Zhang et al. 2009; Persson and Halle 2008b; Grossman et al. 2011; Nucci et al. 2011b; Armstrong et al. 2011; Pal et al. 2002).

This distinct modulation of hydration dynamics compared to that of bulk water is not only observed on protein surfaces and interfaces but also on the surface and

across the lipid bilayers. ODNP has revealed a longer range gradient than previously assumed, in the translational dynamics of hydration water across the normal of the lipid membrane, from the bilayer center reaching at least up to ~ 20 Å above the phosphate group off the lipid bilayer surface (Cheng et al. 2013). Thus, when proteins bind to the lipid membrane, this hydration dynamics gradient can be used as a ruler to obtain information about the binding, orientation, immersion depth, and secondary structure of the membrane associating proteins under physiological conditions. Here, protein residues that may be declared simply “solvent-exposed” by other characterization methods, such as solution-state NMR or power-saturation EPR, can exhibit meaningful variations in their local solvent environment by ODNP that can translate into variation in spatial location (Cheng et al. 2013). Thus, ODNP, in conjunction with various EPR techniques, including cw EPR lineshape analysis (Hubbell et al. 2000; Bordignon 2012), pulsed dipolar EPR (Jeschke 2012; Georgieva et al. 2008) and power-saturation EPR (Columbus and Hubbell 2002; Altenbach et al. 1994; Jao et al. 2008), provide a complementary approach to study the structure, dynamics, and function of proteins under physiological conditions with site-specific resolution. The strength of EPR-based techniques and ODNP is that large and complex protein systems can be investigated at physiological conditions. In this chapter, we review the theory and recent applications of ODNP for the study of protein hydration in solution. We discuss advances, limitations, and promises of the ODNP method, as well as future prospects for its applications and developments.

2 Methodology

ODNP (Overhauser 1953) relies on exploiting the fast decaying dipolar interactions between the nuclear spin and the electron spin within 10 Å distance of each other, and thus can capture local dynamics of the nuclear spin if the spin probe is localized, e.g., on biomolecular surfaces. If the nuclear spin of interest is the ^1H of water in the hydration layer of these biomolecular surfaces, quantification of the ODNP rates can provide information on the local hydration dynamics. Here, we review the theoretical background of ODNP, the data analysis, and assumptions needed to extract the hydration dynamics information in solution samples.

2.1 Theory of ODNP in Solution

When two spins I and S are dipolar coupled in a static magnetic field B_0 , their interaction can be described by the Hamiltonian H ,

$$H = -\gamma_s \hbar (\vec{S} \cdot \vec{B}_0) - \gamma_I \hbar (\vec{I} \cdot \vec{B}_0) - \gamma_s \gamma_I \hbar^2 \left[\frac{3(\vec{I} \cdot \hat{r})(\vec{S} \cdot \hat{r})}{r^3} - \frac{\vec{I} \cdot \vec{S}}{r^3} \right] \quad (1)$$

if the scalar coupling between the I and S spins is negligible.¹ γ_S and γ_I are the gyromagnetic ratio for spins S and I , respectively, while r is the distance between the two spins. \tilde{r} is the unit vector along the center-to-center direction of the two spins. The first two terms in Eq. (1) are Zeeman terms, H_0 , that induce energy splitting of the spin states in the static magnetic field, and the third in Eq. (1) is the dipole-dipole interaction term, H_1 . In the case of nitroxide spin labels interacting with the ^1H nuclei of water (see Fig. 1a), the gyromagnetic ratio for the electron S spin is 28.0 GHz/T (Weil and Bolton 2007) and for the ^1H I spin is 42.6 MHz/T (Lide 2004).

For a nuclear spin I with a spin quantum number $1/2$ (assuming the spin S to be absent) in a static magnetic field of B_0 , the number of up-spins with quantum number $1/2$, n_+ , and down-spins with quantum number $-1/2$, n_- , changes with the strength of magnetic field, according to the Boltzmann distribution. The nuclear spin polarization P_0 is defined as

$$P_0 = \frac{n_+ - n_-}{n_+ + n_-} = \frac{e^{\gamma_I \hbar B_0 / 2k_B T} - e^{-\gamma_I \hbar B_0 / 2k_B T}}{e^{\gamma_I \hbar B_0 / 2k_B T} + e^{-\gamma_I \hbar B_0 / 2k_B T}} \quad (2)$$

where k_B is the Boltzmann constant, and T is the temperature. For ^1H spins at room temperature, spin polarization P_0 is $\sim 10^{-6}$ in a static magnetic field of 0.35 T. In thermal equilibrium, spins relax from n_+ state to n_- state and from n_- state to n_+ state with their relaxation rates, while the polarization remains constant over time. Relaxation rate from n_+ state to n_- state and relaxation rate from n_- state to n_+ state differ only by $n_+ - n_- \sim 2 P_0$. Therefore, practically, both relaxation rates are the same and noted as w^0 .

When S spins² with spin quantum number $1/2$ are introduced to the local environment of the I spin, the 4 energy eigenstates of the unperturbed Hamiltonian H_0 are as shown in Fig. 1a. Let's denote w_0 as the transition rate at which spins I and S change in opposite direction, so that the total spin quantum number change is 0, and w_2 as the transition rate at spins I and S change in the same direction, so that the total spin quantum number change is 2. Similarly, w_1 can be defined as the transition rate at which spin I changes its spin state, while spin S stays at the same spin state, so that the total spin quantum number change is 1³. Likewise, p is noted for the transition rate for only spin S to change its state. In the pool of I and S spins, the macroscopic magnetic moments of I and S spins, $\langle I_z \rangle$ and $\langle S_z \rangle$ in the direction of the applied static magnetic field can be expressed as the difference in the number of spin states with I spin up and S spin up N_{++} , I spin down and S spin up N_{-+} , I spin up and S spin down N_{+-} , and both spins down N_{--} , as follows (Solomon 1955):

$$\begin{aligned} (N_{++} + N_{+-}) - (N_{-+} + N_{--}) &= K \langle I_z \rangle \\ (N_{++} + N_{-+}) - (N_{+-} + N_{--}) &= K \langle S_z \rangle \end{aligned} \quad (3)$$

¹ This condition is valid if I is proton and S is electron.

² Here, S spin typically represents electron spin of nitroxide radical for ODNP

³ w_0 , w_1 and w_2 are denoted as nuclear-electron zero-, single-, and double-quantum transition rates.

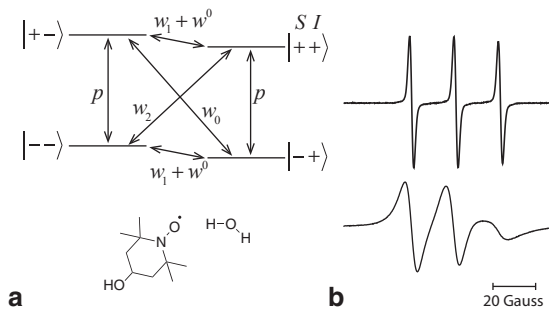


Fig. 1 **a** Four-level energy diagram for a coupled electron (S) and proton (I). Structures of 4-hydroxyl-TEMPO nitroxide radical and water are shown below. **b** An EPR spectrum of 2 mM nitroxide spin radical free in water (*above*). The rotational correlation time of the spin label side chain is much less than 100 ps. An EPR spectrum of 2 mM nitroxide spin radical tethered at the phosphocholine (POPC) vesicle surface (*below*). Its rotational correlation time is on the order of nanoseconds due to the spatial restriction of phosphate headgroups of lipid vesicles

where K is a system-dependent constant. Brackets represent the ensemble average.

From the definition of the transition rates w , the number of spin states change with time as

$$\begin{aligned}
 \frac{dN_{++}}{dt} &= -(w_1 + w^0 + p + w_2)N_{++} + pN_{+-} + (w_1 + w^0)N_{-+} + w_2N_{--} + C_1 \\
 \frac{dN_{+-}}{dt} &= pN_{++} - (w_0 + w_1 + w^0 + p)N_{+-} + w_0N_{-+} + (w_1 + w^0)N_{--} + C_2 \\
 \frac{dN_{-+}}{dt} &= (w_1 + w^0)N_{++} + w_0N_{+-} - (w_0 + w_1 + w^0 + p)N_{-+} + pN_{--} + C_3 \\
 \frac{dN_{--}}{dt} &= w_2N_{++} + (w_1 - w^0)N_{+-} + pN_{-+} - (w_1 + w^0 + p + w_2)N_{--} + C_4.
 \end{aligned} \tag{4}$$

The constants C_1 – C_4 are introduced to match the equilibrium spin states as expressed in Eq. (2). Combining Eqs. (3) and (4), the time evolution of the magnetization is expressed with the following Bloch equations for macroscopic magnetization of the I and S spins,

$$\begin{aligned}
 \frac{d\langle I_z \rangle}{dt} &= -(w_0 + 2w_1 + w_2 + 2w^0)(\langle I_z \rangle - I_0) - (w_2 - w_0)(\langle S_z \rangle - S_0) \\
 \frac{d\langle S_z \rangle}{dt} &= -(w_2 - w_0)(\langle I_z \rangle - I_0) - (w_0 + 2p + w_2)(\langle S_z \rangle - S_0),
 \end{aligned} \tag{5}$$

where I_0 and S_0 are the equilibrium magnetization of spins I and S in the absence of dipolar coupling, respectively.

When the relaxation of S spin is dominated by the radiation-driven transitions induced by the microwave field, where the change in electron spin polarization $\langle S_z \rangle$ is not governed by Eq. (5), and at steady state where $d\langle I_z \rangle / dt = 0$, the magnetization

of the I spins $\langle I_z \rangle$ can be solved from the $d\langle I_z \rangle / dt$ part of Eq. (5) as follows (Hausser and Stehlik 1968):

$$\begin{aligned} \langle I_z \rangle &= I_0 + \frac{w_2 - w_0}{w'} (S_0 - \langle S_z \rangle) \\ &= I_0 \left(1 + \frac{w_2 - w_0}{w_0 + 2w_1 + w_2} \cdot \frac{w_0 + 2w_1 + w_2}{w'} \cdot \frac{S_0 - \langle S_z \rangle}{S_0} \frac{S_0}{I_0} \right), \end{aligned} \quad (6)$$

where the total relaxation rate $w' = 1/T_1 = w_0 + 2w_1 + w_2 + 2w^0$ is defined as the inverse of the nuclear longitudinal relaxation time. Note that $2w^0$ is the inverse nuclear longitudinal relaxation time in the absence of spin S , $1/T_{10}$, and the other w terms in Eq. (6) are the transition rates in the presence of S spin and induced by the dipolar coupling. Equation (6) is further simplified as (Hausser and Stehlik 1968)

$$\langle I_z \rangle = I_0 \left(1 - \xi f s \left| \frac{\gamma_s}{\gamma_I} \right| \right), \quad (7)$$

with the coupling factor ξ , leakage factor f , and saturation factor s defined as follows:

$$\begin{aligned} \xi &\equiv \frac{w_2 - w_0}{w_0 + 2w_1 + w_2} = \frac{\sigma}{\rho} \\ f &\equiv \frac{w_0 + 2w_1 + w_2}{w'} = \frac{\rho}{\rho + 2w^0} = 1 - \frac{T_1}{T_{10}} \\ s &\equiv \frac{S_0 - \langle S_z \rangle}{S_0} \end{aligned} \quad (8)$$

For electron spin S and nucleus spin I , γ_s/γ_I is 657, so that the nuclear magnetization is enhanced in the presence of the I - S dipolar coupling. $\sigma = w_2 - w_0$ is the I - S dipolar cross-relaxation rate, and $\rho = w_0 + 2w_1 + w_2$ is the total dipolar self-relaxation rate of the I spins induced by the presence of S spins.

The dipolar coupling Hamiltonian H_I can be treated as a perturbation to the unperturbed energy eigenstates. If $|m_i\rangle$ and $|m_j\rangle$ are the two energy eigenstates of the unperturbed Hamiltonian H_0 corresponding to energies E_i and E_j , the transition probability per unit time between the two states is (Solomon 1955)

$$w_{ij} = \frac{1}{t\hbar^2} \left| \int_0^t \langle m_j | H_I(t) | m_i \rangle e^{-i\omega_{ij}t} dt \right|^2, \quad (9)$$

where $w_{ij} = (E_j - E_i)/\hbar$. With the help of the Pauli spin operators for spin 1/2, $I_{x,y,z}$, and spin creation and annihilation operator $I_{\pm} = I_x \pm iI_y$, the dipolar coupling Hamiltonian H_I is decomposed into (Bloembergen et al. 1948)

Protein NMR

Modern Techniques and Biomedical Applications

Berliner, L. (Ed.)

2015, X, 185 p. 68 illus., 37 illus. in color., Hardcover

ISBN: 978-1-4899-7620-8